

Conduction-band dispersion, critical points, and unoccupied surface states on GaAs(110): A high-resolution angle-resolved inverse photoemission study

D. Straub, M. Skibowski,* and F. J. Himpsel

IBM Thomas J. Watson Research Center, P.O. Box 218, Yorktown Heights, New York 10598

(Received 8 March 1985)

We report the first angle-resolved, high-resolution inverse photoemission study of the cleaved (110) surface of GaAs. The dispersion of the lowest conduction bands along the Γ - K - X main symmetry direction has been measured using inverse photoemission spectroscopy with tunable electron energy for initial energies between 10 and 30 eV. The photon spectra can be explained by direct optical interband transitions if bulk umklapp processes are taken into account. The Γ_{15} critical point is found at 4.8 eV above the valence-band maximum. The maximum of the Γ_1X_1 band is seen at 3.5 eV and the saddle of the Σ_1 band from Γ_{15} to X_5 has been measured at 6.2 eV. In the center of the surface Brillouin zone at $\bar{\Gamma}$ a surface resonance is located at 2.1 eV above the valence-band maximum in the conduction band. The surface state shows noticeable downward dispersion with k_{\parallel} of -0.4 eV in the direction toward \bar{X} and little dispersion of -0.1 eV toward \bar{X}' .

INTRODUCTION

During the last two decades of semiconductor research, GaAs has evolved as a prototype material for the whole class of III-V compound semiconductors, materials that have been of continuously growing technical and scientific interest in recent years. Direct band gaps and high mobilities make these materials well suited for semiconductor devices operating at high speed¹ or in optical applications,² but major unsolved problems concerning passivation and contacting have hindered a large-scale application up to now. Despite huge efforts, we have not yet achieved a full understanding of the properties of the clean surface and the surface-vacuum interface, which is an essential step for understanding Schottky-barrier formation and oxidation at the surface.

Although the (100) surface is continuously used in technology,³ the (110) surface is the most studied surface of GaAs. It is the only nonpolar surface and can be prepared easily *in situ* as it is the natural cleavage plane. The (110) surface differs significantly from the ideally terminated bulk crystal. It shows surface relaxation with the As atoms moving outward and the Ga atoms moving into the surface to obtain a more planar sp^2 configuration.⁴ The electronic bulk energy bands of GaAs have been a subject of many theoretical⁵ and experimental studies. The occupied electronic states of III-V semiconductors are well understood and have been measured extensively by photoemission,⁶⁻¹¹ but little is known about the unoccupied states.

Concerning empty electronic states of III-V compound semiconductors, research has focused on the existence and exact energetic position of surface and interface states in the band gap. Using partial-yield photoelectron spectroscopy (PYS), an empty surface state was found which appeared to be located in the middle of the fundamental band gap.¹²⁻¹⁴ Early contact-potential-difference measurements¹⁵ showed a Fermi-level pinning on n -type

GaAs at midgap, presumably due to those unoccupied surface states, supporting, therefore, the PYS results. Theoretical calculations for an unrelaxed (110) surface¹⁶⁻²⁰ agreed quite well and also predicted empty surface states in the middle of that band gap. The picture was marred, however, by the very careful and previously unnoticed work-function measurements of van Laar *et al.*,²¹ who showed that the Fermi-level pinning at midgap on GaAs(110) is due to cleavage defects and that there are no intrinsic empty surface states in the fundamental band gap. The PYS results had to be reinterpreted^{22,23} by suggesting the existence of a surface exciton with an unusual high binding energy of at least 0.5 eV, and theoretical calculations for a relaxed surface showed that the empty surface state is moved into the conduction band upon relaxation.²⁴⁻²⁹ Theoretical calculations also showed that the occupied surface states respond comparatively insensitively upon different relaxation models (although the difference between the unreconstructed and reconstructed surfaces was very significant),²⁵ whereas the empty surface states vary much more significantly to different reconstructions. Previous optical³⁰ and energy-loss^{21,31,32} measurements gave some insight into the existence of empty surface states by probing transitions between occupied and unoccupied states, but left the point in momentum (\mathbf{k}) space at which the transition takes place, and the final-state energy, undetermined. Furthermore, excitonic effects cannot be ruled out for these measurements as well.

The bulk band structure of GaAs has been extensively studied by a large number of optical spectroscopies. The valence bands have been carefully mapped by angle-resolved photoemission spectroscopy.^{3,8-11} Interband optical transitions at critical points have been measured with an accuracy of better than a few tenths of meV's.³³ By combining the transition energies with the initial-state valence-band energies from photoemission, the position of conduction-band critical points can, in principle, be in-

ferred. Obviously, the reliability of the conduction-band energies depends on the correct location of interband transitions in k space, which is not always unambiguously possible. It is thus desirable to have an independent determination of conduction-band energies and dispersions. Inverse photoemission reveals the momentum and energy of unoccupied states directly via the time-reversed photoemission process.^{34,35} This has been recently used to map conduction bands for Si,³⁶ Ge,³⁷ and GaP,³⁸ and will be presented below for GaAs. Our measurements also shed some light on the more fundamental question as to how reasonable the common interpretation of photoelectron spectra and optical excitations in the one-electron energy scheme is. Strictly speaking, photoelectron spectroscopy measures ionization energies, whereas inverse photoemission measures the energy $h\nu$ that is released as a photon when an electron undergoes a transition from an initial state E_i into an unoccupied final state with energy $E_f = E_i - h\nu$. E_f is thus the energy of an electron affinity level. The sum of binding and optical transition energies differs from the affinity levels by the exciton energy E_x for the electron-hole interaction. Recently reported values for E_x have been 0.5 and 0.25 eV for the E_1 and E'_1 optical transitions in silicon, respectively.³⁶ For germanium a 0.15-eV excitonic lowering of the E_1 valence-to-conduction-band transition is conceivable.³⁷

A previous inverse photoemission study³⁹ on ion-bombarded and annealed GaAs(110) was focused on the position of empty surface states. It showed no emission tailing into the bulk band gap and gave no indication of empty surface states in the fundamental gap. This earlier study was performed in the angle-integrated mode and, therefore, revealed only density-of-states $[N(E)]$ information. It has a lower resolution of 0.8 eV full width at half maximum (FWHM) and depended strongly on the numerical decomposition of bulk and surface contributions in the spectra.

It is the purpose of the present investigation to elaborate upon these earlier measurements using high-resolution inverse photoemission in order to determine the position of the empty surface state more accurately and to give some insight into the dispersion of the surface-state band with k_{\parallel} . We, furthermore, want to map the anti-bonding sp conduction bands below the vacuum level along the $\Gamma\Sigma K SX$ main symmetry direction which have been inaccessible to photoemission measurements. The binding energy of the surface exciton for transitions from the Ga $3d_{5/2}$ surface core level into the surface state can be obtained and some information can be given on excitonic effects for optical determination of bulk critical points.

The paper is organized as follows: After a brief description of the apparatus and sample preparation, we present the analysis of normal-incidence inverse photoemission spectra for various initial electron energies E_i in terms of conduction-band dispersion along the $\Gamma\Sigma K SX$ direction of GaAs Brillouin zone. The next section describes our results on the surface-state energy and dispersion, and relates our results to optical and energy-loss measurements for the GaAs(110) surface. Finally, we give a brief summary of our main results.

EXPERIMENTAL

The inverse photoemission spectra were measured using a newly developed spectrometer which uses a fast $f/4$ grating monochromator with simultaneous detection of the whole photon spectrum between 8 and 30 eV by two position-sensitive devices which cover the ranges 8–20 eV and 16–30 eV, respectively.^{40,35} The electrons are emitted from an electron gun in the Pierce-type geometry with a low-temperature BaO cathode and impinge under variable angles onto the sample surface. Energy and momentum resolution are typically 0.3 eV and 0.1 \AA^{-1} , respectively, and are mainly limited by the thermal spread of the electrons. The energy $h\nu$ of the emitted photon is measured for a chosen initial electron energy E_i , the latter being referenced to the sample Fermi level E_F . The spectra to be discussed show the photon intensity versus the final-state energy E_f , which has been calculated according to $E_f = E_i - h\nu$. The photon-energy calibration of the spectrometer was obtained experimentally from the high-energy cutoff of spectra from evaporated gold films and from the hydrogen Lyman- α radiation.

GaAs has the fcc zinc-blende crystal structure with a lattice constant $a = 5.65 \text{ \AA}$. The important main symmetry direction for this investigation is the $[110] \Gamma\Sigma K SX$ direction, which has a length of $\sqrt{2}(2\pi/a) = 1.57 \text{ \AA}^{-1}$ from Γ to X . The samples used were $(4 \times 4 \times 15)\text{-mm}^3$ bars of p -type Zn-doped ($n_A = 1.7 \times 10^{18} \text{ cm}^{-3}$) GaAs oriented by x-ray methods prior to cutting. The bars were cleaved in a separate preparation chamber in a vacuum of better than 1×10^{-10} Torr along $[\bar{1}10]$ or $[001]$ to expose (110) surfaces of high quality and mirrorlike finish. The preparation facilities include low-energy electron diffraction (LEED), a retarding-field Auger arrangement, and a Kelvin probe for work-function measurements. Immediately after the cleave, the samples were transferred under vacuum into the measurement chamber, where the vacuum was better than 5×10^{-11} Torr during data acquisition. Multiple cleaves were checked after the inverse photoemission experiment by LEED, and all exhibited a sharp 1×1 diffraction pattern. To avoid charging and uncontrolled voltage drops at the interface between sample and sample holder, two indium contacts were alloyed into the back of the sample bar. The Ohmic behavior of those contacts was confirmed by I - V measurements. A voltage drop in the surface region was not observed. For well-cleaved surfaces one has a flatband situation without depletion layer,⁴¹ and our oxygen coverages are low enough to avoid significant band bending.

The Fermi-level position at the surface can be directly derived from the conduction-band low final-energy onset of our spectra. Different surface Fermi-level positions due to defects or surface contamination on the cleaved surfaces could be seen as a rigid shift of the whole photon spectra. From our data for a very good cleave, shown in Fig. 1, we obtained an onset at $E_f = 1.3 \text{ eV}$, which is equivalent to a Fermi-level pinning at 0.1 eV above the valence-band maximum (VBM). Within our experimental accuracy, this is compatible with previously reported values.^{21,42} Small shifts of the Fermi-level position of typically less than 100 meV upon the low oxygen cover-

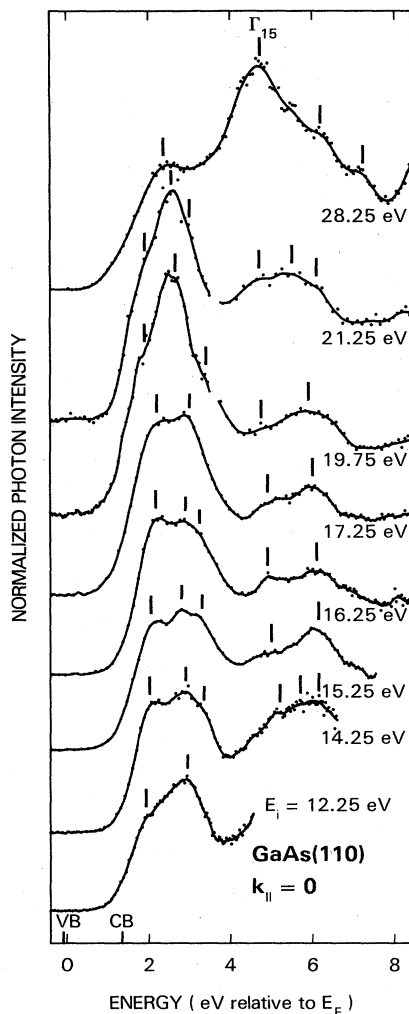


FIG. 1. Normal-incidence inverse photoemission spectra from cleaved GaAs(110) for different initial electron energies E_i . The tick marks indicate the spectral features that are further discussed in the text and assigned to conduction-band transitions in Fig. 2.

ages (< 0.1 layer) used in this study were corrected by lining up bulk related spectral features in the photon spectra from clean and oxygen-exposed surfaces. The size of these shifts is in good agreement with the ones reported in Ref. 42 for low oxygen exposures.

RESULTS AND DISCUSSION

Bulk band structure

Figure 1 shows a series of inverse photoemission spectra obtained with the electron beam impinging perpendicularly onto the GaAs(110) surface ($\hbar k_{\parallel} = 0$). Each spectrum represents the sum over data from different cleaves and is normalized to the deposited charge. The spectra

display the energy distribution of the emitted photons for a given initial energy E_i of the incident electron ranging from 12.25 to 28.25 eV. The energy scale is given relative to the Fermi level for a perfect cleave, and the positions of the valence-band maximum and conduction-band minimum are also indicated. The spectrum for $E_i = 28.25$ eV and the lower final-energy part of the two spectra for $E_i = 21.25$ and 19.75 eV are obtained from the high-energy photon detector, which has superior resolution in the high-photon-energy range (see experimental section and Ref. 40). The spectra shown were recorded from a variety of surfaces with different cleavage quality for an extended time of data acquisition, and they show primarily bulk features with the surface-state features (see below) being suppressed.

Three distinct features can be distinguished in the measured spectra. A multiplet peak shows up between 2 and 3.5 eV. For initial electron energies of about 20 eV this multiplet reduces into a doublet with a highly dominating peak around 2.6 eV. A second peak at about 4.7 eV above E_F is most pronounced in the 28.25-eV spectrum. This peak decreases in intensity and disperses upwards for the lower initial energies. A third peak is well resolved at about 6 eV in the 17.25-eV spectrum. It shows noticeable dispersion and can be seen in all spectra. Most of these tick-marked structures reflect transitions into conduction bands and can be interpreted in the direct-transition scheme.

The direct-transition model describes the inverse photoemission process as interband optical transitions under energy and momentum conservation and has been used successfully to interpret GaAs(110) photoemission results from $h\nu \leq 8$ eV (Ref. 43) up to 100 eV (Refs. 7 and 8). For the transition of an electron through the vacuum-solid interface, only the electron momentum parallel to the surface $\hbar k_{\parallel}$ is conserved, and in order to map the final inverse photoemission bands we have to know the initial-state-band dispersion and, in particular, the momentum perpendicular to the surface $\hbar k_{\perp}$ for a given electron energy. A generally used approximation is the description of the higher conduction bands as free-electron-like bands. Their dispersion can then be described by

$$E_i(\mathbf{K}) = \frac{\hbar^2}{2m} (\mathbf{k} + \mathbf{G})^2 - E_0, \quad (1)$$

\mathbf{K} being the total wave vector, \mathbf{k} the wave vector in the reduced Brillouin zone, and \mathbf{G} a lattice vector of the reciprocal lattice. The influence of the crystal is approximated by the inner potential E_0 . Reference for all energies is the valence-band maximum. For normal incidence, i.e., $\hbar k_{\parallel} = 0$, Eq. (1) reduces to a description for the electron momentum perpendicular to the sample surface,

$$\hbar k_{\perp}(E_i) = \sqrt{(2m)(E_i - E_0)^{1/2} - \hbar G_{\perp}}, \quad (2)$$

G_{\perp} being the component of \mathbf{G} perpendicular to the surface.

In the more general case of off-normal incidence, i.e., for nonvanishing $\hbar k_{\parallel}$, only the momentum parallel to the sample surface is conserved in a transition through the vacuum-solid interface. Knowing the angle of electron incidence θ and the sample work function Φ , this com-

ponent of the momentum can be calculated according to the following relation:

$$\hbar k_{\parallel}(E_i) = \sqrt{2m}(E_i - \Phi)^{1/2} \sin\theta. \quad (3)$$

In Ref. 11 the dispersion $E(k_{\parallel})$ of the conduction bands above the vacuum level has been mapped along $\Gamma\Sigma K SX$ for InAs using photoemission spectroscopy. This study showed that the final photoemission states (i.e., the initial inverse photoemission states) cluster around a free-electron-like parabolic band with $\mathbf{G}=[000]$ in the expanded-zone scheme, which is equivalent to $\mathbf{G}=[220]$ in the reduced-zone scheme, and resembles the normal free-electron band in the $[110]$ direction with no umklapp involved. However, this study also showed that significant contributions of direct interband transitions also stem from two initial bands far away in \mathbf{k} space from this simple free-electron parabola.

Using the results of a similar study for GaAs(110),⁴⁴ we were able to obtain a value of -9.8 eV for E_0 by adjusting the free-electron parabola to the experimentally mapped conduction bands in the middle between the zone boundaries where the perturbation by the crystal potential can be expected to be smallest. This is in good agreement with the theoretically calculated bottom of the muffin-tin potential at -9.34 eV,⁸ and a previous experimental value of -8.0 eV obtained at photon energies above 30 eV.⁸

The only two other significantly contributing bands (see Fig. 2) can be easily reproduced by using $\mathbf{G}=[\bar{1}11]$ and $\mathbf{G}=[00\bar{2}]$ and their associated energy degenerate partners in formula (2). The deviation of these idealized bands from the experimentally mapped ones is generally less than 0.25 \AA^{-1} for $\mathbf{G}=[00\bar{2}]$ and virtually vanishes for $\mathbf{G}=[\bar{1}11]$ and the free-electron-like parabola.

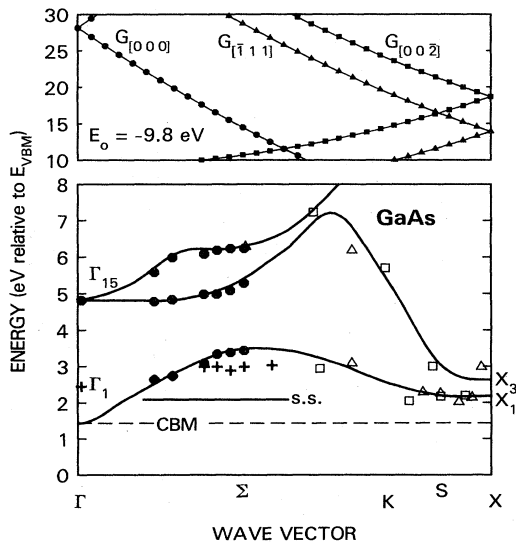


FIG. 2. Energy dispersion of conduction band states along $\Gamma\Sigma K SX$ as derived from inverse photoemission data. The upper panel shows the initial free-electron-like bands with the umklapp vectors involved as parameters. The solid line labeled s.s. indicates the position of the surface resonance as derived by contamination-dependent measurements.

The topology of the three lowest conduction bands of III-V compound semiconductors is well established. Therefore, we had almost no problems assigning the strongest features in the measured spectra to direct transitions from the free-electron-like parabola. Weaker peaks were tested to see whether they could be reasonably positioned in \mathbf{k} space if this free-electron initial band was used. If this possibility had to be discarded, a possible umklapp was considered. The result of this $E(k_{\parallel})$ assignment is summarized in Fig. 2. In the upper panel of this figure the calculated initial bands are shown with the used bulk umklapp vectors \mathbf{G} as parameter. The lower panel shows the experimentally obtained conduction-band structure along $\Gamma\Sigma K SX$. The most pronounced tick-marked features in Fig. 1 can generally be assigned to direct transitions from the free-electron band with $\mathbf{G}=[220]$ (solid dots). Note that for $E_i=28.25$ eV the optical transition takes place very close to the Γ point and that a very pronounced peak at 4.7 eV is found in the spectrum. This peak can unambiguously be assigned to transitions into the Γ_{15} symmetry point in analogy with photoemission results which exhibit a strong transition from the occupied Γ_{15} point at this photon energy. The strength of this transition is due to the flatness of the bands around Γ_{15} and a high transition cross section for p states, respectively. The spin-orbit splitting of 0.17 eV at this point³⁵ is below our resolution and therefore cannot be resolved.

However, no strong transitions into the Γ_1 point are found. A likely explanation is a low cross section due to the s character of this band at Γ and the shape of the band there, resulting in a small density of states. The transitions from the occupied Γ_1 states are found to be weak in photoemission as well.^{8,9} The slightly dispersing peak at 6.2 eV resembles the Σ_1 band from Γ_{15} to an X_5 point at about 13 eV and in close proximity to the saddle point of this band. The various overlapping peaks below 3.5 eV are more difficult to assign. A tentative explanation can be derived from the very pronounced peaks in (17.25–21.25)-eV spectra around 2.6 eV, which are probably due to direct transitions from the free-electron band into the lowest conduction band. This band can then be pursued through the low-energy spectra as less pronounced peaks.

The remaining structural features are due to transitions involving surface states and a $[\bar{1}11]$ (open triangles) or a $[00\bar{2}]$ umklapp (open squares). Note that the main effect of both umklapps is to position the observed direct transitions closer to the X point of the GaAs Brillouin zone. Therefore, it is conceivable that an alternative interpretation of these features in a one-dimensional density-of-states picture would lead to identical results.

There is only one feature left, at approximately 2.9 eV, which does not fit into the direct-transition model, marked by plus signs in Fig. 2. A possible explanation is that it is due to a one- or three-dimensional density of states $[N(E)]$. This is further supported by theoretical calculations. A recent self-consistent density-of-states calculation shows a strong peak in the density of states shortly below 3 eV,⁴⁵ which can be found at comparable energies in many calculations. Another confirmation of the $N(E)$ nature of this structure is given in Fig. 3, show-

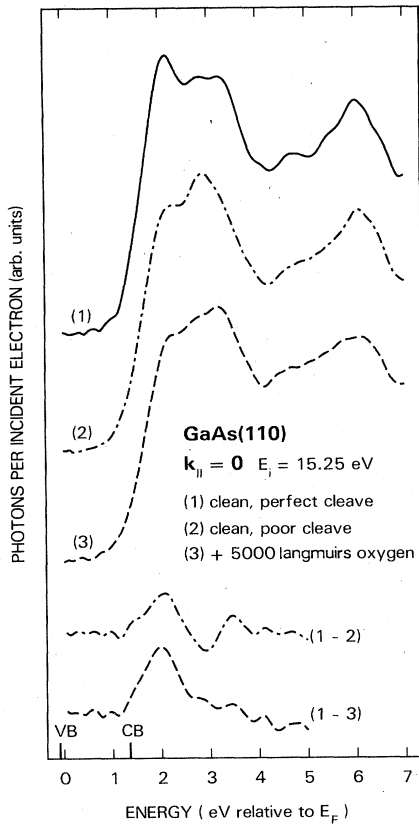


FIG. 3. Normal-incidence inverse photoemission spectra for $k_{\parallel}=0$ and $E_i=15.25$ eV. The data from a perfect cleave (solid line) exhibit a surface resonance at 2.0 eV above E_F which is weak for a poor cleave (2) and after oxygen contamination (3). On a poor cleave (dashed-dotted line) one peak at 2.9 eV is emphasized which is assigned to a maximum in the bulk density of states.

ing this to be the dominant peak in the low-energy part of the spectrum for a very poor cleave. There, a strong perturbation of the incoming electron wave at steps and defect sites is conceivable, and contributions from a large part of the Brillouin zone many contribute to the inverse photoemission spectrum. Similar effects have been reported for photoemission in Ref. 46.

Referring the energy values of our results to the valence-band maximum, we find (4.8 ± 0.1) eV for Γ_{15} , (6.3 ± 0.1) eV for the Σ_1 saddle point, and (3.5 ± 0.1) eV for maximum of the lowest conduction band. By combining valence-band positions with optical transition energies, in Ref. 8 a value of 4.77 eV is derived for the energy of the Γ_{15} critical point. Thus, we find no indication of excitonic effects for the optical valence- to conduction-band transitions into Γ_{15} within our error margin of ± 0.1 eV for the determination of the critical-point energy.

Surface states

A close look at the empty surface states can be taken in Fig. 3, which shows bremsstrahlung spectra at normal in-

cidence ($\hbar k_{\parallel}=0$) and an electron energy of 15.25 eV. The solid line, labeled (1), displays the spectrum obtained for a clean and perfectly mirrorlike surface. This spectrum exhibits all the structures discussed in the preceding subsection. The influence of different surface conditions can be seen in the two other inverse photoemission spectra, (2) and (3), respectively. The dashed-dotted spectrum (2) was taken for a very poor cleave with a high density of steps. To account for the different Fermi levels on this surface, the whole spectrum has been shifted energetically by 50 meV using the well-pronounced bulk peak at 6 eV as a guideline. Spectrum (3) (dashed line) was taken after an oxygen exposure of 5000 L (Ref. 47) to the perfect cleave of spectrum (1) ($1 \text{ L}=1 \text{ langmuir}=10^{-6} \text{ Torr sec}$). This exposure corresponds to not more than 0.1 monolayer of oxygen coverage and results in a Fermi-level shift of 50 meV.⁴² In the lower part of Fig. 3 difference spectra are drawn to further illuminate the influence of the surface conditions on the spectra.

The main feature in the difference spectra occurs at 2.0 eV, where a well-resolved peak on the perfect and clean surface is strongly suppressed on the two other surfaces. We assign this structure to the Ga-derived empty dangling-bond surface state. All other structures remain virtually unchanged by the various surface treatments and are, therefore, assigned to the bulk contributions already discussed in the preceding subsection.

Off-normal inverse photoemission spectra are shown in Figs. 4 and 5. Angle of incidence and electron energy were chosen after Eq. (3) to measure close to high-symmetry points of the surface Brillouin zone, which is

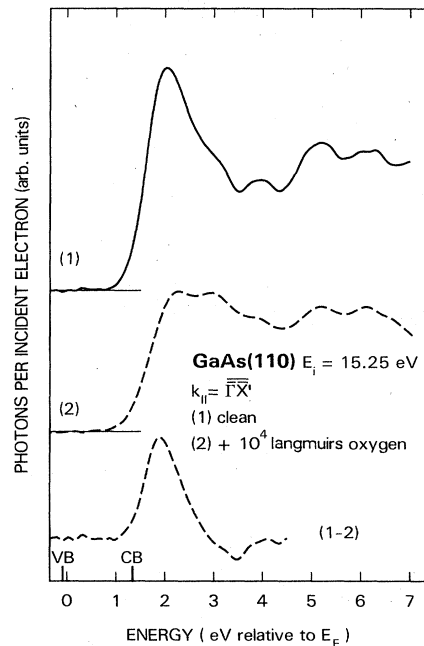


FIG. 4. Off-normal inverse photoemission spectra for clean and oxygen-contaminated surfaces with $k_{\parallel}=0.56 \text{ \AA}^{-1}$ along [001], which corresponds to the \bar{X}' symmetry point of the surface Brillouin zone.

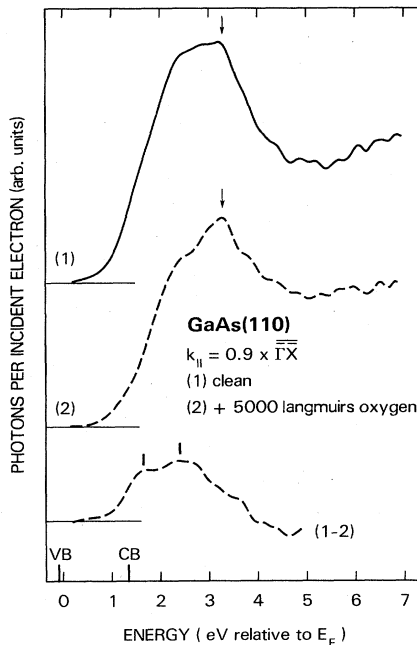


FIG. 5. Off-normal inverse photoemission spectra for clean and oxygen-contaminated surface with $k_{\parallel} = 0.71 \text{ \AA}^{-1}$ along $[\bar{1}10]$, which corresponds to $0.9\bar{1}\bar{X}$. The arrow-marked peak is due to transitions into the lowest bulk conduction band.

displayed in Fig. 6. The surface contribution to the spectra was derived in a fashion similar as for normal electron incidence by controlled oxygen contamination of the clean surface. Figure 4 shows a very pronounced surface state at 1.9 eV above E_F , indicating only minor dispersion with k_{\parallel} along $\bar{1}\bar{X}$. In the $\bar{1}\bar{X}$ direction, the shorter dimension of the surface unit cell in real space, there occurs a possible doublet of surface states at 1.65 and 2.4 eV above E_F . This indicates a noticeable downward dispersion of 0.4 eV from $\bar{1}$ to \bar{X} . Our findings on the empty-surface-state dispersion are summarized in Fig. 7, which also shows the measured occupied surface bands taken from Ref. 48. Also shown are the possible optical transitions at

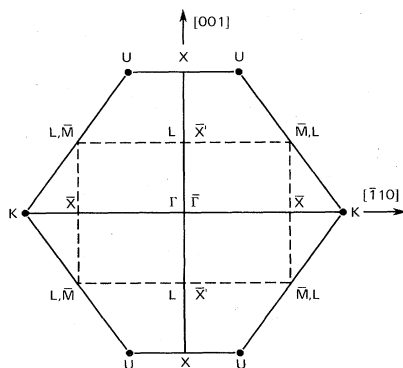


FIG. 6. Surface Brillouin zone $\bar{1}\bar{X}\bar{M}\bar{X}$ of GaAs(110) (dashed line) and the underlying projection of the bulk Brillouin zone.

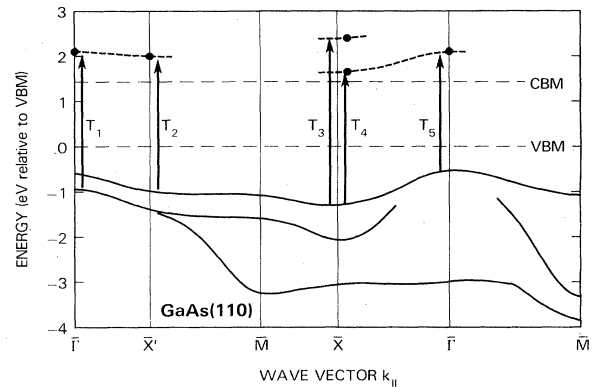


FIG. 7. Experimental surface band structure of GaAs(110). The occupied surface bands are taken from Ref. 48. Solid dots indicate the results of this investigation and the arrows show possible direct transitions from filled to empty surface states, which can explain optical and energy-loss data.

the measured high-symmetry points from occupied into unoccupied surface states, the transition energies being T_1 – T_5 . We find the lowest transition energy to be 2.7 eV in the zone center at $\bar{1}$. The possible transition energies cluster around 3.0 eV (T_1 , T_2 , and T_4). An additional transition is found at $T_3 = 3.8$ eV. A 3-eV-wide energy gap between occupied and empty surface states over a substantial part of the surface Brillouin zone is in almost perfect agreement with the 3.1-eV surface-related transition found in energy-loss spectra.^{21,32,32} Optical spectroscopy³⁰ at the GaAs(110) surface shows the onset of surface-related transitions well above 2.6 eV with maxima at 2.9, 3.2, and 3.8 eV. This is also compatible with our empirical surface band structure shown in Fig. 7. The remaining energy differences of the order of 0.1 eV between the optical and energy-loss data, and our energy levels in combination with the bands from Ref. 48, could be due to excitonic effects in the surface-related transitions. However, we want to mention that 0.1 eV is well within the combined error margins of our experiment and the photoemission data of Ref. 48.

In electron-energy-loss spectroscopy^{21,31,32} and photoemission-yield spectroscopy,^{12–14} a Ga $3d_{5/2}$ core-level-to-surface-state transition is found at 19.68 eV with the binding energy of the Ge $3d_{5/2}$ surface core level being 18.88 eV.⁴⁹ This positions the final state for the transition at 0.80 eV above the VBM. Finding the empty surface state at least at 1.75 eV above the valence-band maximum, we can deduce a minimal binding energy of 0.95 eV for the surface exciton. This is compatible with a very rough recent estimate of 0.8 eV given in Ref. 49 and in perfect agreement with the value of 0.96 eV reported for the GaP(110) surface.³⁸ A more detailed analysis of our data with respect to excitonic binding energies is given in Ref. 50.

SUMMARY

The results of our high-resolution inverse photoemission study of GaAs(110) can be summarized as follows:

(i) The band dispersion of the lower unoccupied bands of GaAs has been mapped for the first time. In particular, the p -like antibonding Γ_{15} point has been determined, which is the antibonding counterpart of the valence-band maximum.

(ii) The precise energy locations of the unoccupied Ga-derived surface states have been measured.

(iii) Our results for unoccupied states can be combined with previous photoemission measurements in order to predict optical and electron-energy-loss transitions. The difference between predicted and actual energies can be ascribed to the electron-hole interaction. We find that the electron-hole interaction is negligible for valence to conduction-band transitions, both in the bulk and at the

surface. For core to conduction-band transitions at the surface, the electron-hole interaction is substantial and an accurate value of 0.95 eV is obtained for the Ga 3d-to-unoccupied-surface-state transition.

ACKNOWLEDGMENTS

The authors want to thank L. Ley for helpful discussions and comments. We thank G. Lapeyre for sending us his unpublished data and A. Marx for his expert technical support. One of us (M.S.) wishes to thank IBM for making possible his fruitful stay at the IBM Thomas J. Watson Research Center.

- *Permanent address: Universität Kiel, D-8300 Kiel, Federal Republic of Germany.
- ¹P. M. Solomon and H. Morkoç, *IEEE Trans. Electron. Devices ED-31*, 1015 (1984).
- ²A. Y. Cho, *J. Vac. Sci. Technol.* **16**, 275 (1979).
- ³P. K. Larsen, J. F. Van der Veen, A. Mazur, J. Pollmann, J. H. Neve, and B. A. Joyce, *Phys. Rev. B* **26**, 3222 (1982).
- ⁴C. B. Duke, *Appl. Surf. Sci.* **11-12**, 1 (1982), and references therein.
- ⁵See, for example, N. E. Christensen, *Phys. Rev. B* **30**, 5753 (1984); G. B. Bachelet and N. E. Christensen, *ibid.* **31**, 879 (1985), and references therein.
- ⁶L. W. James and J. L. Moll, *Phys. Rev.* **183**, 740 (1968); W. E. Spicer, and R. C. Eden, in *Proceedings of the IXth International Conference on the Physics of Semiconductors, Moscow, 1968* (Nauka, Leningrad, 1968).
- ⁷J. A. Knapp, D. E. Eastman, K. C. Pandey, and F. Patella, *Bull. Am. Phys. Soc.* **23**, 399 (1978).
- ⁸T. C. Chiang, J. A. Knapp, M. Aono, and D. E. Eastman, *Phys. Rev. B* **21**, 3515 (1980).
- ⁹T. C. Chiang and D. E. Eastman, *Phys. Rev. B* **22**, 2940 (1980).
- ¹⁰M. Skibowski *et al.* (unpublished).
- ¹¹G. P. Williams, F. Cerrina, J. Anderson, G. J. Lapeyre, R. J. Smith, J. Hermannson, and J. A. Knapp, *Physica* **117&118B**, 350 (1983).
- ¹²D. E. Eastman and J. L. Freeouf, *Phys. Rev. Lett.* **33**, 1601 (1974).
- ¹³W. E. Spicer, I. Lindau, P. E. Gregory, C. M. Garner, P. Pianetta, and P. W. Chye, *J. Vac. Sci. Technol.* **13**, 780 (1976).
- ¹⁴J. C. McMenamin and R. S. Bauer, *J. Vac. Sci. Technol.* **15**, 1262 (1978).
- ¹⁵J. H. Dinan, L. K. Galbraith, and T. E. Fischer, *Surf. Sci.* **26**, 587 (1971).
- ¹⁶C. Bail and D. J. Morgan, *Phys. Status Solidi B* **50**, 199 (1972).
- ¹⁷J. D. Joannopolous and M. L. Cohen, *Phys. Rev. B* **10**, 5075 (1974).
- ¹⁸C. Calandra and G. Santoro, *J. Phys. C* **8**, L86 (1975).
- ¹⁹C. Calandra and G. Santoro, *J. Phys. C* **9**, L51 (1976).
- ²⁰J. R. Chelikowsky and M. L. Cohen, *Phys. Rev. B* **13**, 826 (1976); **14**, 556 (1976).
- ²¹J. van Laar and J. J. Scheer, *Surf. Sci.* **8**, 234 (1967); A. Huijser and J. van Laar, *ibid.* **52**, 202 (1975); A. Huijser, J. van Laar, and T. L. van Rooy, *ibid.* **62**, 472 (1977); J. van Laar, A. Huijser, and T. L. van Rooy, *J. Vac. Sci. Technol.* **14**, 894 (1977).
- ²²G. J. Lapeyre and J. Anderson, *Phys. Rev. Lett.* **35**, 117 (1975).
- ²³W. Gudat and D. E. Eastman, *J. Vac. Sci. Technol.* **13**, 831 (1976).
- ²⁴K. C. Pandey, *J. Vac. Sci. Technol.* **15**, 440 (1978).
- ²⁵D. J. Chadi, *J. Vac. Sci. Technol.* **15**, 631 (1978).
- ²⁶D. J. Chadi, *Phys. Rev. B* **18**, 1800 (1978).
- ²⁷J. R. Chelikowsky and M. L. Cohen, *Solid State Commun.* **29**, 267 (1979).
- ²⁸A. Zunger, *Phys. Rev. B* **22**, 959 (1980).
- ²⁹M. Schmeits, A. Mazur, and J. Pollmann, *Phys. Rev. B* **27**, 5012 (1983).
- ³⁰P. Chiaradia, G. Chiarotti, F. Ciccacci, R. Memeo, S. Nannarone, P. Sassaroli, and S. Selci, *Surf. Sci.* **99**, 70 (1980); P. Chiaradia, G. Chiarotti, F. Ciccacci, R. Memeo, S. Nannarone, P. Sassaroli, and S. Selci, *J. Phys. Soc. Jpn.* **49**, 1109 (1980).
- ³¹R. Ludeke and A. Koma, *J. Vac. Sci. Technol.* **13**, 241 (1976).
- ³²H. Lüth, M. Büchel, R. Dorn, M. Liehr, and R. Matz, *Phys. Rev. B* **15**, 865 (1977).
- ³³*Landoldt-Börnstein, Zahlenwerte und Funktionen aus Naturwissenschaften und Technik, Neue Serie* (Springer-Verlag, Berlin, 1982), Vol. III, 17a, p. 220.
- ³⁴V. Dose, *Prog. Surf. Sci.* **13**, 225 (1983); J. B. Pendry, *J. Phys. C* **14**, 1381 (1981); N. V. Smith, *Vacuum* **33**, 803 (1983).
- ³⁵F. J. Himpsel and Th. Fauster, *J. Vac. Sci. Technol. A* **2**, 815 (1984).
- ³⁶D. Straub, L. Ley, and F. J. Himpsel, *Phys. Rev. Lett.* **54**, 142 (1985).
- ³⁷D. Straub, L. Ley, and F. J. Himpsel (unpublished).
- ³⁸D. Straub, M. Skibowski, and F. J. Himpsel, *J. Vac. Sci. Technol. A* **3**, 1484 (1985).
- ³⁹V. Dose, H.-J. Gossmann, and D. Straub, *Phys. Rev. Lett.* **47**, 608 (1981); *Surf. Sci.* **117**, 387 (1982).
- ⁴⁰Th. Fauster, D. Straub, J. J. Donelon, D. Grimm, A. Marx, and F. J. Himpsel, *Rev. Sci. Instrum.* **56**, 1212 (1985).
- ⁴¹For p -type GaAs usually a flat-band situation is found for well-cleaved surfaces: see also Ref. 22.
- ⁴²G. Landgren, R. Ludeke, Y. Jugnet, J. F. Morar, and F. J. Himpsel, *J. Vac. Sci. Technol. B* **2**, 351 (1984).
- ⁴³D. L. Rogers and C. Y. Fong, *Phys. Rev. Lett.* **34**, 660 (1975).
- ⁴⁴G. J. Lapeyre (private communication).
- ⁴⁵C. S. Wang and B. M. Klein, *Phys. Rev. B* **24**, 3393 (1981).
- ⁴⁶F. Cerrina, J. R. Myron, and G. J. Lapeyre, *Phys. Rev. B* **29**, 1978 (1984).
- ⁴⁷As the ion gauge was operating during the oxygen exposure,

we expect to have "excited" oxygen in the preparation chamber.

⁴⁸A. Huijser, J. van Laar, and T. L. van Rooy, *Phys. Lett.* **65A**, 337 (1978).

⁴⁹D. E. Eastman, T. C. Chiang, P. Heimann, and F. J. Himpsel, *Phys. Rev. Lett.* **45**, 656 (1980).

⁵⁰M. Skibowski, D. Straub, and F. J. Himpsel (unpublished).